

## STUDY OF THE PROCESS OF BREAKING ROLLED STEEL BY BENDING FOR STAMPING UNDER IMPACT AND COMBINED LOADING

Karnaikh S. G., Markov O. Ye.

### INTRODUCTION

At the present stage of mechanical engineering development, the problem of energy resources and metal economical use during its processing specifies ever increasing requirements to technology and equipment for separating raw materials into workpieces. This requires the development of already known and the creation of new effective separation processes and equipment for their implementation<sup>1</sup>.

At every engineering enterprise, the rolled stock separating is typical and massive. Considering that ten millions of workpieces from rolled stock are produced every month in the world, the relevance of works aimed at improving the existing and developing new technologies for the production of workpieces becomes evident. Among the known methods of separating of rolled stock into dimensional workpieces, used in modern procurement production, the most productive and economical ones are waste-free methods of separating rolled stock. They are cutting by shearing and cold breaking by bending. During this time, a large amount of material has been accumulated on the destruction nature, mechanisms and criteria<sup>2</sup>. The following scientists made a significant contribution to the development of this science: K. Kessler, O. Keller, T. Nakagawa, T. Ekobori, E. Orovan, G. V. Kolosov, M. I. Muskhelishvili, G. I. Barenblatt, M. Ya. Leonov, S. O. Khristianovich, G. P. Cherepanov, V. V. Panasyuk, O. I. Tselikov, K. M. Bogoyavlensky, V. G. Kononenko, V. M. Finkel, V. T. Meshcherin, V. P. Romanovsky, S. S. Solovtsov, N. L. Lisunets, V. A. Timoshchenko and many others<sup>3</sup>.

### 1. Analysis of literature data and goal setting

In this paper, a method of separating rolled stock using cold breaking by bending is considered. The idea of the method consists in a preliminary stress

---

<sup>1</sup> Tang B., Liu Y., Mao H. Investigation of a novel modified die design for fine-blanking process to reduce the die-roll size. *Procedia Engineering*. 2017. №207, P. 1546–1551. doi:10.1016/j.proeng.2017.10.1076.

<sup>2</sup> Joun M. S., Jeong S. W., Park Y. T., Hong S. M. Experimental and numerical study on shearing of a rod to produce long billets for cold forging. *Journal of Manufacturing Processes*. 2021. №62. P. 797–805. doi: 10.1016/j.jmapro.2020.12.062.

<sup>3</sup> Lisunets N. L. Usage of physical and mathematical simulation for improvement of the processes of metal shear cutting. *CIS Iron and Steel Review*. 2019. №17. P. 34–38.

concentrator applying to the rolled stock and bending of the rolled stock until it breaks in the stress concentrator. A brittle crack in terms of its potential is an ideal tool for waste-free separation of solid materials into parts. At the same time, the energy consumption for cutting is approaching to its minimum possible theoretical level<sup>4</sup>. However, the widespread adoption of this separation method is hindered by the unstable nature of crack propagation. This leads to a low quality of the resulting workpieces.

The development and application of effective methods of destruction control can significantly improve the method of breaking of rolled stock into workpieces and also create fundamentally new methods suitable for obtaining workpieces for machining. They are based on understanding the reasons leading to undesirable fracture deviations from a given trajectory. This allows to propose effective ways to improve the quality of the resulting surface.

Promising trends for improving breaking by bending are increasing the loading rate and creating a complex stress state that impedes plastic flow in the fracture area. The papers shows that an increase in the loading rate changes the behavior of the metal and also the nature of plastic deformation and fracture, the stress-strain state of the metal, the ratio of the plastic stage and the stage of destruction, the shape and size of the deformation zone. This ensures the minimum possible level of plastic deformation, which precedes the initiation of the main crack, and low energy consumption of the process.

However, in the process of shock loading at high rates, the bending of the specimen is accompanied by elastic deformations and vibrations at the contact with the supports and the tool. In this case, the fracture process becomes uncontrolled due to the instability of the crack trajectory<sup>5</sup>. Insufficient information about the causes of this phenomenon and possible methods of dealing with it contributes to the belief that supercritical destruction is an uncontrolled process. It cannot be used for high-quality separating of rolled stock into workpieces<sup>6</sup>. This is explained, among other things, by the complexity of describing the destruction dynamics, and by the prevailing disproportion between the development of theoretical and experimental methods for studying the cracks propagation in dynamic fracture mechanics.

It is also necessary to take into account the inertial loads arising from the displacement and rotation of the specimen halves in the process of separation using the method of breaking by bending.

---

<sup>4</sup> Lisunets N. L. Improving the efficiency of the processes of billets manufacture from rolled metal via shift cutting based on simulation. *Chermye Metally*. 2018. №6. P. 31–35.

<sup>5</sup> Karnaukh S. G., Markov O. E., Aliieva L. I., Kukhar V. V. Designing and researching of the equipment for cutting by breaking of rolled stock. *International Journal of Advanced Manufacturing Technology*. 2020. № 109. P. 2457–2464. DOI: <https://doi.org/10.1007/s00170-020-05824-7>.

<sup>6</sup> Zheng Q., Zhuang X., Zhao Z. State-of-the-art and future challenge in fine-blanking technology. *Production Engineering*. 2019. №13. P. 61–70.

To solve this problem, it is proposed to load the specimen with a static force before separation. This allows to provide the initial displacement of the specimen in contact with the supports and to reduce the vibration of the specimen and the tool. The possibility of preliminary static loading in combination with a high deformation rate allows to create a complex stress state scheme in the specimen, which provides the required geometric accuracy and quality of the resulting workpieces.

In the papers<sup>7</sup>, mathematical models of the specimen separation in the plane of the stress concentrator are proposed. Existing design models have been developed for impact tests on pendulums and hammers, when the mass of the movable tool is much greater than the mass of the specimen. In this case, during impact, there is no significant reduction in the speed of the moving parts. On a press-hammer, the mass of the intermediate punch can be commensurate with the mass of the specimen. Therefore, it is necessary to take into account the change in the punch speed during loading.

In the papers<sup>8</sup>, the well-known model of specimens' impact testing for concentrated bending with an elastic-plastic hinge was used. In the study of plastic flow in the separation plane at three-point bending, conclusions are drawn. Despite the change in the zone of plastic deformation, with an increase in the angle of rotation in the central region, a rigid zone is formed, bounded by the shear strain rate rupture lines. With respect to this zone, which is an elastic-plastic hinge, the halves of the specimen rotate. The known model is applicable only for cold bending breaking, when the angle of the specimen rotation halves before fracture is small and brittle fracture occurs through crack propagation without significant plastic deformation.

Analysis of the known fracture models and the proposed complex model of specimen fracture establishes that the behavior of a crack depends on a number of uncontrolled factors. The task becomes more complicated with dynamic and static-dynamic loading, when it is extra necessary to take into account the influence of the equipment design parameters.

The papers<sup>9</sup>, consider numerical modeling of experiments to determine the dynamic crack resistance of materials. It is shown that for impact testing of specimens according to the three-point bending scheme, a significant simplification of the procedure for determining the basic solutions is possible.

---

<sup>7</sup> Karnaukh S. G., Karnaukh D. S. Research of the influence of deformation speed on energy and power adjectives of the process of three-point cold bend breaking and on alignment integrity of raw parts. *Metallurgical and Mining Industry*. 2011. №3. P. 107–114.

<sup>8</sup> Karnaukh S. G., Karnaukh D. S. Research of the influence of deformation speed on energy and power adjectives of the process of three-point cold bend breaking and on alignment integrity of raw parts. *Metallurgical and Mining Industry*. 2011. №3. P. 107–114.

<sup>9</sup> Карнаух С. Г., Бігунов О. О., Мучник О. Є. Дослідження процесу статико-динамічного навантаження зразків за схемою триточкового холодного ламання згином на прес-молотах. *Машинознавство*. 2000. №12. С. 31–36.

This becomes possible when using the theories of Euler – Bernoulli or Timoshchenko. In this case, the presence of a crack is modeled by introducing an additional angle of rotation in the corresponding section. The data obtained with this approach correlate adequately with the experimental data, which also testifies in favor of the chosen model of impact tests with a flexure hinge.

The papers<sup>10</sup> presents a complex mathematical model of the specimen static-dynamic loading according to the scheme of three-point bending on a press-hammer with the same direction of deforming forces. It differs from the known models by taking into account the preliminary static loading and design features of the press-hammer. In this case, at the moment of impact, the speed of the tool is equal to the speed of the moving parts. On press-hammers, the mass of the intermediate punch can be comparable to the mass of the specimen, and its speed at the moment of impact is equal to zero. The intermediate punch accelerates upon impact simultaneously with the deformation of the specimen; therefore, it is necessary to take into account the change in the punch speed during loading.

The purpose of the work is to improve the quality of workpieces obtained by breaking rolled stock by studying the separation process under dynamic and static-dynamic loading on a press-hammer.

## **2. Mathematical modeling of the dynamic and static-dynamic breaking of rolled stock according to the three-point bending scheme**

Dynamic and static-dynamic loading of rolled stock can be carried out on a press-hammer. The Fig. 1 shows a diagram of the static-dynamic loading of specimens according to the three-point bending scheme on a press-hammer. The press-hammer has the following advantages: the ability to create quasi-static, shock and combined loads in a wide range of rates, energies and forces; precise metering of energy and force during deformation of the rolled stock, etc.<sup>11</sup>

Dynamic loading of the specimen 6 is carried out by a hydroelastic cylinder, which uses a previously compressed liquid as an energy accumulator. The pump (Fig. 1, b) creates pressure in the working chamber 8 of the hydroelastic cylinder. When a predetermined pressure value is reached, the control cavity 9 is cut off from the overflow and connected to the pumping under pressure.

---

<sup>10</sup> Karnaukh S. G., Aliiev I. S. Research of process of division of grade rolling on the measured blanks by method of breaking bend at static and shock loading. *Scientific journals of Vinnitsa national agrarian university. Engineering, energy, transport*. 2021. Vol.112, № 1. C. 81–87. doi: 10.37128/2520-6168-2021-1-10.

<sup>11</sup> Karnaukh S. G., Markov O. E., Kukhar V. V., Shapoval A. V. Research of the rolled stock separating into workpieces using breaking by bending with dynamic and static-dynamic force. *The International Journal of Advanced Manufacturing Technology*. 2022. №120. P. 2763–2776. doi: 10.1007/s00170-022-08902-0.

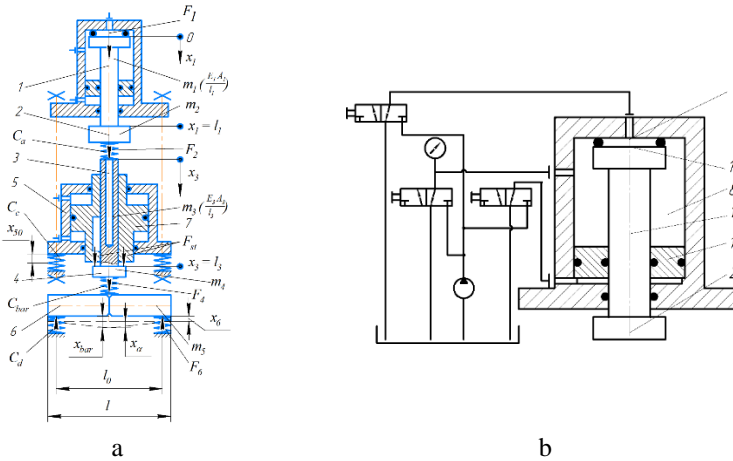


**Fig. 1. Schematic diagram of a press-hammer: a – calculation scheme of specimen with dynamic and static-dynamic loading by the method of cold breaking by bending on a press-hammer; b – construction diagram of a press-hammer hydroelastic cylinder**

There is a loss of sealing in the control cavity 9. The working fluid under high pressure affects the whole area of the top end 10 of the rod 1. The rod 1, together with the head 2, is rapidly moving down. At the same time, it loads the intermediate punch 3 with a punch 4, installed along the axis of the hydraulic cylinder 5 (Fig. 1, a). Under the shock loading, the specimen 6 is broken by bending.

To implement the static-dynamic loading mode, a plunger 7 is provided in the design of the press-hammer (see Fig. 1, a). The plunger 7 moves under the action of high fluid pressure in the hydraulic cylinder 5 and acts on the end face of the punch 4. In this case, a preliminary static loading of the specimen 6 occurs in the same direction with its final separation. After that, dynamic (shock) loading of the specimen 6 occurs before fracture. The press-hammer cycle is reproduced.

The movement of the rotating parts (see Fig. 1, a) occurred under the action of the drive force  $F_1 = f[U_1(x_1 = 0)]$ , where  $U_1$  is the rod movement the section  $x_1$ . Intermediate punch 3 with the mass  $m_3$  was presented in the form of a variable cross-section rod with parameters  $A_3(x_3)$ , elasticity modulus  $E_3$ , length  $l_3$ , and punch 4 had the form of the concentrated mass  $m_4$ . The impact time 1... 2 ms is small as compared to the period of natural longitudinal oscillations of the intermediate punch section. Therefore, for the correctness of the mathematical model, it is necessary to take into account the wave processes occurring in the intermediate punch. Since the length of the

punch  $l_3$  is commensurate with the length of the rod  $l_1$ . It was assumed that the dependence of the change in force at the contact between head 2 and intermediate punch 3 on deformation  $F_2 = f_2(\Delta_2)$  is nonlinear. Linearized stiffness of the contact between head 2 and intermediate punch 3 –  $C_a = const$ . Technological force  $F_4 = f_4(\Delta_4)$  is applied in the middle to specimen 6 with mass  $m_4$ , located on two supports. The element stiffness  $C_{bar} = const$  reflects the elastic properties at the contact of the specimen with the punch. Two symmetric elements with stiffness  $C_d = const$  simulate the elastic properties in the contact of the supports with the specimen and act on the specimen by  $F_6$  forces. Such modeling of the supports influence on the specimen by two equal forces  $F_6$  is coherent with experiment. In the static-dynamic loading mode at the first stage, the specimen 6 with the stiffness  $C_{bar} = const$  is loaded by the static force  $F_{st}$  of the hydraulic cylinder 5, which causes deformation of the engine bed elements, which has the stiffness  $C_c = const$ .

The proposed complex model of the specimen static-dynamic loading according to the scheme of three-point bending on a press-hammer, partially used the well-known model of specimen impact testing for concentrated bending with an elastic hinge, characterized by the presence of initial deformations of sections under the action of a preliminary static force. A specimen of  $m_5$  mass was presented in the form of two rigid halves connected to each other by an elastic hinge, the rotation angle  $\alpha$  of which is proportional to the bending moment  $M_{curv}$  in the central section:

$$M_{curv} = \alpha \cdot l_0^2 \cdot (8 \cdot C_{bar}), \quad (1)$$

where  $\alpha$  – rotation angle of specimen halves;  
 $l_0$  – distance between supports;  
 $E$  – elasticity modulus of specimen material;  
 $C_{bar}$  – static stiffness of the specimen:

$$C_{bar} = d \cdot E / (\lambda \cdot (a/d)), \quad (2)$$

where  $d$  – specimen diameter;  
 $E$  – elasticity modulus of specimen material;  
 $\lambda$  – dimensionless specimen calibration factor;  
 $a$  – crack length.

The equation of motion for an arbitrary section of masses  $m_1, m_3$  is:

$$\partial^2 U_i / \partial t^2 = c_i^2 \cdot [(1/A_i) \cdot (\partial A_i / \partial x_i) \cdot (\partial U_i / \partial x_i) + (\partial^2 U_i / \partial x_i^2)], i = 1, 3 \quad (3)$$

where  $U_i$  – section displacement  $i$  – that core;  
 $c_i$  – speed of sound in metal.

The differential equations of concentrated masses motion  $m_2, m_4$ :

$$m_i \cdot (d^2x_i/dt^2) + F_{ai}(\Delta_{ai}) - F_{bi}(\Delta_{bi}) = 0, i = 2,4, \quad (4)$$

where  $x_i$  – mass motion  $m_i$ ;

$F_{ai}(\Delta_{ai}), F_{bi}(\Delta_{bi})$  – forces acting on  $i$  – mass  $m_i$  from the side of the elements in contact with it, located on opposite sides;

$\Delta_{ai}, \Delta_{bi}$  – absolute deformations of the corresponding elastic elements.

For the head –  $m_2$ :

$$F_{a2} = E_1 \cdot A_1 \cdot (\partial U_1 / \partial x_1)|_{x_1=l_1}; \quad (5)$$

$$F_{b2} = f[U_1|_{x_1=l_1} - U_3|_{x_3=0}] \text{ under } U_1|_{x_1=l_1} > U_3|_{x_3=0}, \quad (6)$$

otherwise  $F_{b2} = 0$ , since there is a violation of the contact between the elements of the system, and in the case of a linear dependence

$$F_{b2} = C_a \cdot [U_1|_{x_1=l_1} - U_3|_{x_3=0}]. \quad (7)$$

For the punch –  $m_4$ :

$$F_{a4} = E_3 \cdot A_3 \cdot (\partial U_3 / \partial t)|_{x_3=l_3}; \quad (8)$$

$$F_{b4} = f[U_3|_{x_3=l_3} - x_{bar}] \text{ при } U_3|_{x_3=l_3} > x_{bar}, \quad (9)$$

Otherwise  $F_{b4} = 0$ , and in the case of a linear dependence

$$F_{b4} = C_b \cdot [U_3|_{x_3=l_3} - x_{bar}]. \quad (10)$$

In addition to the equations of the rotating parts and the intermediate punch motion, the equations of forces and moments in the central section were written taking into account the inertial components arising under shock loading. Within the framework of the proposed mathematical model for the specimen deformation according to the three-point bending scheme, we obtain the system of equations

$$\begin{cases} M_{curv} = (m_5 \cdot l \cdot \ddot{x}_{bar}/8) - (m_5 \cdot l^2 \cdot \ddot{\alpha}/24) + (F_6 \cdot l_0/2); \\ F_4 - 2 \cdot F_6 = m_5 \cdot \ddot{x}_{bar} - (\ddot{\alpha}/4 \cdot l \cdot m_5); \\ F_4 = C_{bar} \cdot (x_4 - x_{bar}), \text{ at } x_4 > x_{bar}; \\ F_6 = C_d \cdot (x_{bar} - \alpha/2 \cdot l_0), \text{ at } x_{bar} > \alpha/2 \cdot l_0, \end{cases} \quad (11)$$

where  $l$  – specimen length;

$\ddot{x}_{bar}$  – acceleration of specimen halves;

$\ddot{\alpha}$  – angle acceleration of specimen halves.

After transformations and substitutions, we obtain the system of equations:

$$\begin{cases} \ddot{x}_{bar} = -(6 \cdot l_0 \cdot C_{bar} \cdot x_{bar} / (m_5 \cdot l)) + (C_{bar} \cdot l_0 / (4 \cdot C_a) - l/3 + l_0/2) \times \\ \quad \times 6 \cdot F_6 / (m_5 \cdot l) + F_4 / m_5; \\ \ddot{\alpha} = -(12 \cdot l_0^2 \cdot C_{bar} \cdot \alpha / (m_5 \cdot l^2)) + 24 / (m_5 \cdot l) \times \\ \quad \times (2 \cdot l_0 / l - 1) \cdot F_6 + 12 / (m_5 \cdot l) \cdot F_4. \end{cases} \quad (12)$$

In accordance with the method of initial parameters in the Cauchy form, the displacements of the «press-hammer – specimen» elements in local coordinates were considered. To switch to a common coordinate system, its origin was aligned with the position of the contact point between the specimen and the support before static loading. Then, the initial displacements of the specimen central section –  $x_{bar0}$ , masses  $m_4$ , bed deformation –  $x_{50}$  occurred under the action of the static force  $F_{st}$ . Taking into account the displacement of the rod sections due to the action of the force  $F_{st}$ , the origin of the local coordinate system of the rod was shifted by the value  $(U_{1max} + x_{50})$  so that the movement at the contact between the head and the intermediate punch at the moment of impact was equal to the static one. The total shift of the central section of the specimen was determined as:  $x_{bar} = x_6 + x_\alpha$ .

When solving this problem, the finite difference method was used, which is well suited for similar calculations. The derivatives were approximated by finite differences using a «cross» pattern.

The calculation of the dynamic and static-dynamic cold breaking by bending on a press-hammer of original design was carried out using the developed program «Impactbreaking». Press-hammer parameters: impact energy  $W = 0 \dots 1300 \text{ J}$ ; static drive force  $F_{st} = 0 \dots 100 \text{ kN}$ ;  $F_1 = 0 \dots 12 \text{ kN}$ ;  $F_4 = 0 \dots 80 \text{ kN}$ ;  $m_2 = 2,00 \text{ kg}$ ;  $m_3 = 0,22 \text{ kg}$ ;  $l_1 = 155 \text{ mm}$ ;  $l_3 = 206 \text{ mm}$ ;  $C_a = 100 \dots 500 \text{ MN/m}$ ; speed of moving parts of the press-hammer  $V = 0 \dots 20 \text{ m/s}$ . Specimen parameters:  $d = 16 \text{ mm}$ ;  $l = 76 \text{ mm}$ ;  $l_0 = 60 \text{ mm}$ ;  $E = 2,05 \cdot 10^5 \text{ MPa}$ ;  $m_5 = 0,25 \text{ kg}$ . Calculations were carried out for steel specimens C45 with stiffness in the plane of separation –  $C_{bar} = 5,5 \text{ MN/m}$ , which was determined by calculation by the formula (2).

The way of modeling the contact conditions between the specimen and the supports significantly affects the obtained results. Therefore, based on the available loading scheme and recommendations, it was assumed that the shape of the contact surface of the intermediate punch corresponds to the shape of the supports –  $C_{bar} = C_a = 120 \text{ MN/m}$ .

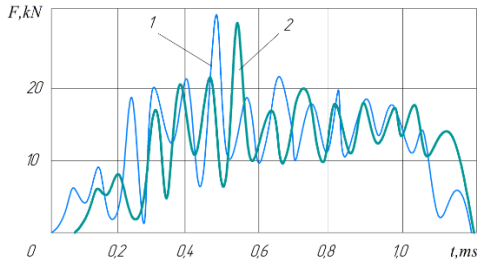
The values of the cross-sectional areas of the rod 1 and the intermediate punch 3 along the length were set in the points ( $i = 0 \dots n$ ) of computational grid ( $n_1 = 31, n_2 = 34$ ), where  $n$  – the number of points.

The influence of the static force  $F_{st}$ , the contact stiffness of the head 2 and the intermediate punch 4 –  $C_a$  on the shape of the change, the amplitude values of the forces  $F_4, F_6$  and the corresponding displacements of the system elements (Fig. 2) was studied.

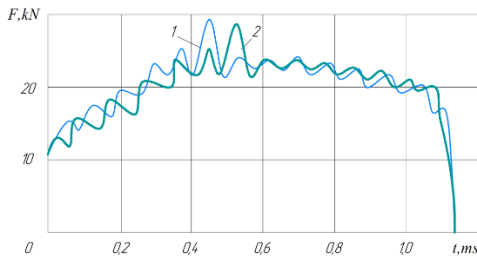


Graph analysis  $F_4 = f(t)$  и  $F_6 = f(t)$  shows, that in the absence of static loading at the initial moment of time, the specimen is detached from the supports (see Fig. 2, a).

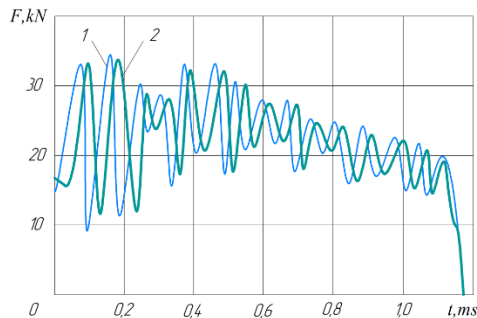
Thus, the loading scheme at the initial time is actually unsupported –  $F_6 = 0$ .



a



b



c

**Fig. 2. Mathematical curves for the forces change in the contact of punch with  $F_4 = f(t)$  and total reaction of supports  $F_6 = f(t)$ :  
a – shock loading  $C_a = 100 \text{ MN/m}$ ; b – static-dynamic loading  $F_{st} = 12 \text{ kN}$ ,  $C_a = 100 \text{ MN/m}$ ; c – static-dynamic loading  $F_{st} = 17 \text{ kN}$ ,  $C_a = 500 \text{ MN/m}$**

The deformation process during three-point bending occurs with bending vibrations of the specimen, which are overlapped with vibrations of a higher frequency, associated with the specimen contact zone compliance to an intermediate punch and supports, and the natural frequency of system elements vibrations.

The presence of a static load  $F_{st}$  at the moment of impact (see Fig. 2, b) leads to a smoother loading of the specimen, sharp peaks of forces on the mathematical curves disappear. An increase in the static component  $F_{st}$  leads to an increase in the amplitude of the forces  $F_4, F_6$  (see Fig. 2, c), although the maximum value of the amplitude for shock loading is higher due to the presence of forces peak values. The averaged forces values  $F_4, F_6$  slightly increase with the growth of the static component  $F_{st}$ .

The value of the static load  $F_{st}$ , necessary to prevent the separation of the specimen 6 from the supports, increases with the increase in the stiffness of the contact between the head 2 and the intermediate punch 3 –  $C_a$  (see Fig. 2, c).

An increase in the static force  $F_{st}$  causes a proportional increase in the initial bending angle of the specimen 6 –  $\alpha$ . This reduces the time  $t_{max}$  to reach the maximum bending angle  $\alpha_{max}$ , the value of which should be limited within  $0,14 \text{ rad}$  to ensure the quality of the resulting workpieces.

Analysis of the graphs  $F_4 = f(t)$  and  $F_6 = f(t)$  for different values of  $C_a$  (see Fig. 2) shows that a decrease in the stiffness of  $C_a$  smoothes the curves. At high values of  $C_a$ , the deformation of the specimen occurs after several collisions of the moving parts with the intermediate punch. The design of the intermediate punch determines its mass and contact stiffness –  $C_a$ . The required compliance of the punch can be ensured by increasing its length, reducing the cross-sectional area due to axial drilling, the shape of the contact surface, and the use of elastic inserts.

### **3. Experimental studies of the separating long products according to the three-point bending scheme under dynamic and static-dynamic loading**

To test theoretical calculations, experimental studies of the separating long products according to the scheme of three-point cold breaking by bending under dynamic and static-dynamic loading were carried out.

For the experiments, the previously considered press-hammer of the original design was applied using the parameters presented above:  $W = 0 \dots 1300 \text{ J}$ ; hydraulic cylinder force 5 (see Fig. 1, a) –  $F_{st} = 0 \dots 100 \text{ kN}$ ;  $V = 0 \dots 20 \text{ m/s}$ ; compressible working fluid volume  $Q = 12 \cdot 10^{-3} \text{ m}^3$ ; working fluid pressure  $p = 0 \dots 18 \text{ MPa}$ ;  $m_2 = 2,00 \text{ kg}$ . The stiffness of the contact between the head and the intermediate punch –  $C_a = 100 \text{ MN/m}$ .

The Fig. 3 shows: the scheme of data registration during experiments (Fig. 3, a): 1 – breaker, 2 – strain indicator, 3 – specimen, 4 – supports;

construction diagram (Fig. 3, b), including photographs of the press-hammer (Fig. 3, c) and equipment (Fig. 3, d).

The installation for separating specimens by the method of cold breaking by bending (see Fig. 3, c) consists of: engine bed 1, in its guides there are breaker mechanisms and supports. The breaker and supports are installed with the possibility of reciprocating movement, limited by detents 2 and straps 3, which are attached to the engine bed 1 with screw-bolts. The position of the clamping mechanism, breaker and supports is fixed using bolts 4 screwed into stops 2, nuts 5 and spacers 6. The breaker mechanism consists of a body 7, the breaker itself 8, installed with the possibility of reciprocating movement in the guides of the body. The support mechanism consists of a body 9 and a supporting plate 10, which is held by a strap 11. Specimen 12 is placed on the supports 10.

The stiffness of contact between breaker 8 and specimen 12 is  $C_{bar} = 120 \text{ MN/m}$ , the rigidity of the specimen 12 contact with the supports 10 is equal to  $C_d = 120 \text{ MN/m}$ .

The information from the strain indicators through the  $E - 440$  universal multi-channel data collection device was fed to a computer, where, after processing using the original program, it was stored in worksheets and graphics convenient for subsequent analysis.

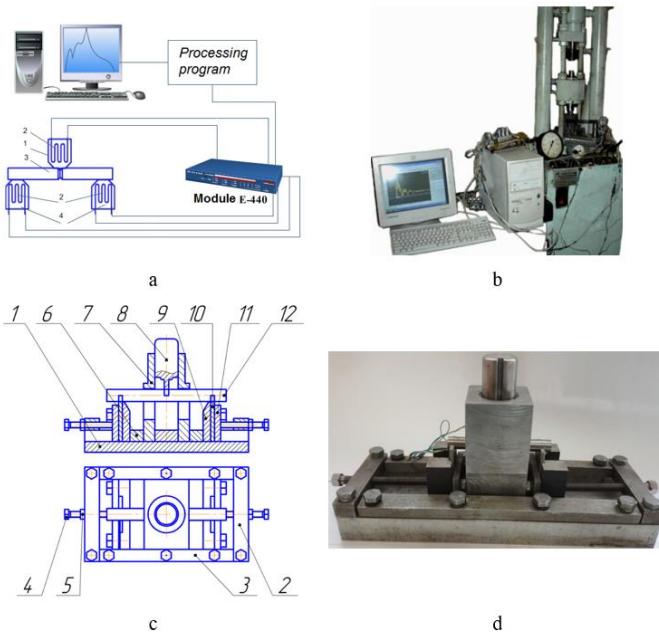


**Fig. 3. The registration scheme of experimental data (a), structural scheme (b) and photographs of experimental equipment (c) and setup (d)**

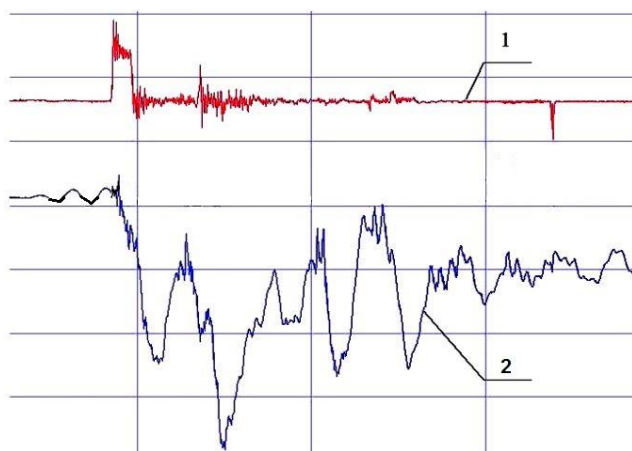
Main characteristics of the  $E - 440$  recorder: digital signal processor  $ADSP - 2185M$  with a clock frequency of  $48\text{ MH}$ ; 16 differential channels or 32 channels with common ground for analog input with automatic zero correction; the maximum operating frequency of the  $14 - \text{bit ADC}$  is  $400\text{ kH}$ , which allows to use this device for studying shock processes.

A several recording channels, signals were simultaneously recorded through two channels: on the breaker and on the supports (see Fig. 3, a).

In the experiment, we used cylindrical specimens with dimensions:  $= 16\text{ mm}$ ;  $l = 76\text{ mm}$ ;  $l_0 = 60\text{ mm}$ ;  $m_5 = 0,25\text{ kg}$ , made of rolled stock from different grades of steel in plastic –  $C20$ , elastoplastic –  $C45$ ,  $37Cr4$  and brittle state –  $60Si7$ .

The specimens were preliminary applied with the stress concentrators in the form of an annular groove of a triangular profile using a turning tool. The following parameters are: depth  $\Delta H = 1,5\text{ mm}$ ; apical radius –  $\Delta r = 0,15\text{ mm}$ . Loading arms –  $30\text{ mm}$ . The sizes of the deformation and fracture zones of the specimens were determined by analyzing the fracture surface using a microscope.

Specimens under dynamic loading were separated by the breaking method according to the three-point bending scheme at the pressure of the working fluid  $p = 15\text{ MPa}$ , which corresponds to the maximum impact speed –  $V = 18\text{ m/s}$ . Typical oscillograms of specimens cold breaking according to the three-point bending scheme under dynamic loading are shown in Fig. 4.



1 – support; 2 – breaker

**Fig. 4. Typical oscillogram of the time dependence on the breaker forces and supports (readings of three channels taken simultaneously) for steel  $60Si7$  (X – axis – time, scale –  $10^5$  measurements in 1 s)**

The smoothed graphs of the change in the force parameters of the three-point bending as a function of time for specimens of different materials under dynamic loading are shown in Fig. 5.

Analysis of the experimental results (see Fig. 5) shows the absence of contact between specimen 15 and supports 13 in the initial phase of loading. The reason for the separation of the specimen from the supports is the inertia of its halves and the high stiffness of the supports with a relatively low stiffness of the specimen.

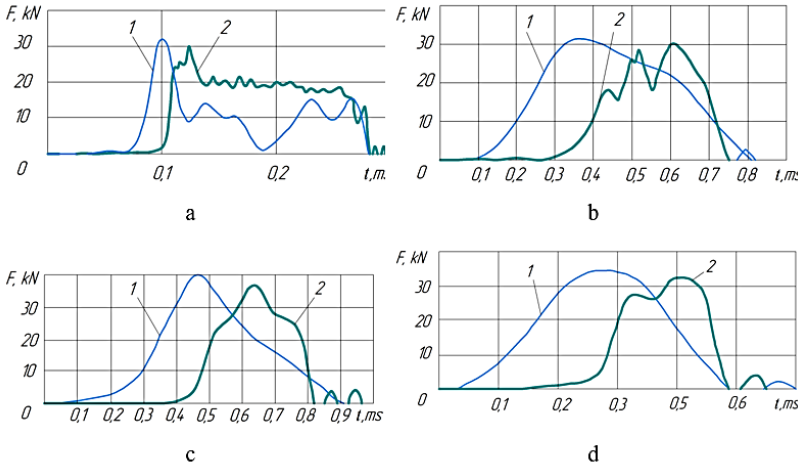


**Fig. 5. Experimental data of the change in forces at the contact of the breaker with the specimen  $F_4 = f(t) - 1$  and total reaction of supports  $F_6 = f(t) - 2$  (readings of two channels taken simultaneously) for steel specimens: a – C20; b – C45; c – 37Cr4; d – 60Si7 under dynamic loading**

This confirms the conclusion that at the initial moment of time the specimen is detached from the supports. Maximum values of forces:  $F_4 \cong 32 \text{ kN}$ ,  $F_6 \cong 30 \text{ kN}$  (steel C45) slightly differ from those calculated above, in accordance with the developed mathematical model:  $F_4 \cong 29 \text{ kN}$ ,  $F_6 \cong 28 \text{ kN}$ . The somewhat overestimated experimental results are explained by a more correct calculation of the specimen stiffness  $C_{bar}$  in the plane of separation and stiffness of the contact between the head and the intermediate punch –  $C_a$ .

The time during which the destruction process occurs for specimens from different steel grades was: C20 –  $t \cong 2,0 \text{ ms}$ ; C45 –  $t \cong 0,8 \text{ ms}$ ; 37Cr4 –  $t \cong 0,9 \text{ ms}$ ; 60Si7 –  $t \cong 0,5 \text{ ms}$ , which corresponds to the design model.

Specimens under static-dynamic loading were separated by the breaking method according to the three-point bending scheme with a preliminary static force  $F_{st} = 12 \text{ kN}$ , the value of which was determined experimentally, taking into account the recommendations.

The smoothed graphs of the change in the force parameters of the three-point bending depending on the time for specimens made of different materials under static-dynamic loading are shown in Fig. 6.

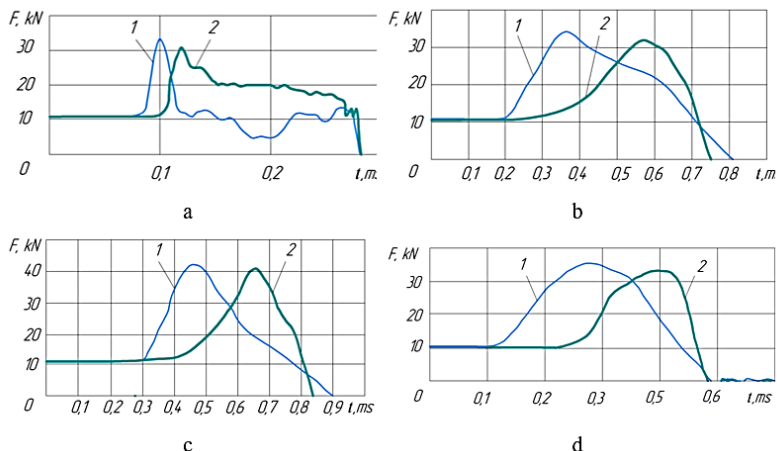


**Fig. 6. Experimental data of changes in forces at the contact of the breaker with the specimen  $F_4 = f(t) - 1$  and total reaction of supports  $F_6 = f(t) - 2$  (readings of two channels taken simultaneously) for steel specimens: a – C20; b – C45; c – 37Cr4; d – 60Si7 under static-dynamic loading**

Analysis of the experimental results (see Fig. 6) shows that the presence of preliminary static loading excludes the separation of the specimen from the supports, which confirms the adequacy of the mathematical model. Preliminary static loading of the specimen on the press-hammer increases its stiffness and ensures its initial displacement at the contact with the supports.

The maximum values of the forces  $F_4$ ,  $F_6$  under static-dynamic loading turned out to be higher in comparison with dynamic loading (Table 1), but not significantly. This is due to the presence of the static component  $F_{st}$ .

The time during which the fracture process occurs for specimens from different steel grades under static-dynamic loading corresponds to the time under dynamic loading.

Table 1

**Experimental measurements of forces  $F_4$ ,  $F_6$  under dynamic and static-dynamic loading**

Steel grade	Separation force at, $kN$			
	dynamic loading		static-dynamic loading	
	$F_4$	$F_6$	$F_4$	$F_6$
C20	32	30	33	31
C45	32	30	34	32
37Cr4	40	38	42	41
60Si7	34	32	36	34

In paper<sup>12</sup>, recommendations were developed for choosing a method for separating rolled bars into cut-to-length blanks according to the value of the values of synergistic criteria: «crack growth criterion» –  $K_{cp}$ , «brittleness criterion» –  $P_{fr}$ . The higher the values of  $K_{cp}$ ,  $P_{fr}$ , the higher the tendency of the material to brittle fracture, and the higher the quality of the blanks obtained during cold bending.

The results of calculations of synergistic fracture criteria for the materials of the samples used in the experiment are presented in Table 2.

Table 2

**Mechanical characteristics of steels and calculated values of fracture criteria**

Steel	$\sigma_{02}$ , $MPa$	$\sigma_B$ , $MPa$	$\delta$ , %	$\psi$ , %	Hard- ness $HB$	$W_c$ , $MJ/m^3$	$K_{ci}$	$K_{cp} \cdot 10^5$ , $(MJ/m^3)^2$	$P_{fr} \cdot 10^8$ , $(MJ/m^3)^3$	$M \cdot 10^3$
C20	250	420	25	55	163	309	1,2	0,58017	0,10878108	3,282
C45	360	610	16	40	197	273	0,8	0,73623	0,19878279	1,395
37Cr4	324	588	14	50	168	345	1,1	0,83739	0,20348584	2,176
60Si7	1175	1270	6	25	269	363	0,3	3,19587	2,81636126	0,174

Table 3 presents the results of calculations of the complex criteria: «crack growth» and «brittleness». These criteria are the basic information attributes. These criteria allow to classify material to next groups: «material in plastic state», «material in elastoplastic state» and «material in brittle state». Based on the analysis of obtained calculations the ranges of values of these criteria for classification of materials by mechanical properties are determined.

<sup>12</sup> Karnaukh S. G., Markov O. E., Kukhar V. V., Shapoval A. V. Classification of steels according to their sensitivity to fracture using a synergetic model. *The International Journal of Advanced Manufacturing Technology*. 2022. №119. P. 5277–5287. DOI: <https://doi.org/10.1007/s00170-022-08653-y>.

Table 3

**Ranges of values of the complex criteria of «crack growth»  
and «brittleness» for groups of materials with different  
mechanical properties**

Steel group	$K_{cp}, (MJ/m^3)^2$	$P_{fr}, (MJ/m^3)^3$
«In plastic state»	$\leq 7 \cdot 10^4$	$\leq 15 \cdot 10^6$
«In elastoplastic state»	$\leq 20 \cdot 10^4$	$\leq 100 \cdot 10^6$
«In brittle state»	$> 20 \cdot 10^4$	$> 100 \cdot 10^6$

The results obtained are in good agreement with the measurements of the geometric accuracy of the specimens obtained experimentally. Photographs of workpieces from different steel grades, separated according to the three-point bending scheme under static and shock loading, are shown in Fig. 7, 8.

Measurement of geometric parameters characterizing the geometric accuracy of the separated specimens was performed by the method of macrostructural analysis by measuring the absolute and relative values of geometric distortions using a universal measuring tool and a microscope.

The results of measurements for the fractal dimensions of workpieces obtained by the method of separating specimens according to the three-point bending scheme under dynamic and static-dynamic loading are shown in Fig. 9, 10.

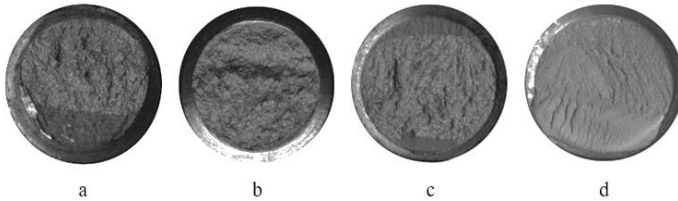


**Fig. 7. Photographs of workpieces obtained under dynamic loading  
by the method of cold bending breaking:  
a – C20; b – C45; c – 37Cr4; d – 60Si7**

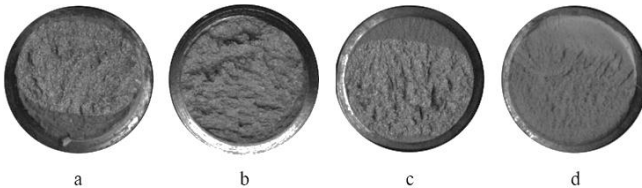


**Fig. 8. Photographs of workpieces obtained under dynamic loading  
by the method of cold breaking by bending:  
a – C20; b – C45; c – 37Cr4; d – 60Si7**



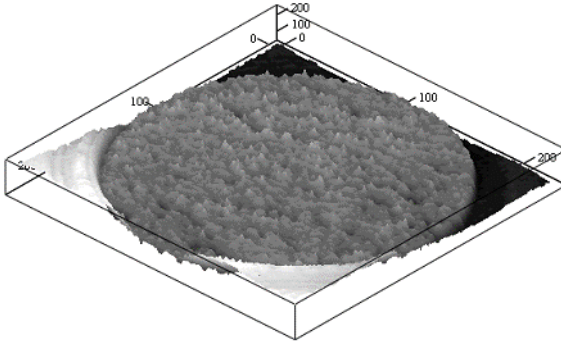


**Fig. 9. Example of measuring fractal dimensions of the workpieces ends made of 60Si7 steel under static-dynamic loading**

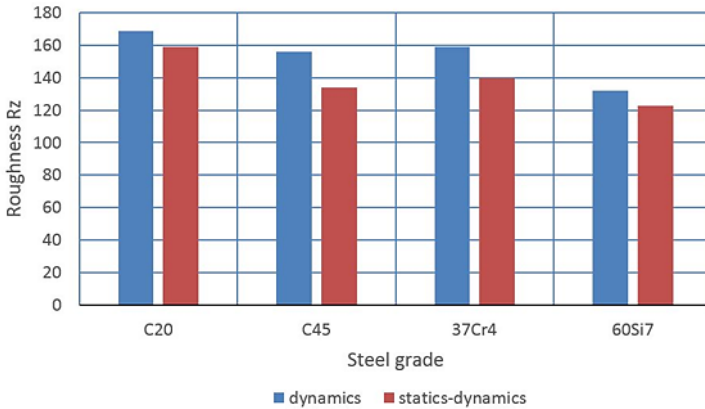


**Fig. 10. Results of workpieces fractal dimensions measurements obtained by the method of separating specimens according to the three-point bending scheme under dynamic and static-dynamic loading**

The analysis of the obtained results shows an improvement in the quality of the specimens under static-dynamic loading as compared to dynamic loading. The highest quality was observed for 60Si7 steel specimens: the fracture is brittle, the fracture surface is brushed, the crack trajectory is straight, and the specimen areas near the stress concentrator are practically not deformed. The roughness of the workpieces ends surface in the plane of separation from steels: 20, C45, 37Cr4 is decreases. The specimens of steel C45 were obtained as a result of viscoelastic fracture, the fracture surface is streaky, rough  $R_z 134$ . The specimens of steel 37Cr4 were obtained as a result of viscoelastic fracture, the fracture surface is streaky, rough  $R_z 140$ . A more

noticeable improvement in the quality of workpieces will be manifested when separating specimens of large cross sections.

The quality of workpieces depends on the efficiency of the stress concentrator applied to the rolled product in the separation plane. There are many ways to apply stress concentrators to rolled products *Ошибка! Залка не определена.* The essence of the method lies in the fact that the energy of elastic deformation of the bed and the drive accumulated in the press during the separation of rolled products, at the moment of destruction, is spent on doing useful work – applying a stress concentrator for breaking by bending the next workpieces.

According to the received charts  $F = f(t)$  (see fig. 5, 6) for specimens from different steel grades with a sufficiently high resolution in both coordinates, the following zones can be distinguished: *I* – crack nucleation zone; *II* – ductile crack growth zone; *III* – brittle destruction zone; *IV* – viscous break zone. Besides, given the high performance characteristics of the system and the possibility of accumulating a large amount of data, it is possible to selectively consider the received signal with a duration of several milliseconds in very narrow time ranges of interest to the researcher (on the order of units and tens of microseconds). This allows to estimate the value of the crack propagation velocity correctly.

For example, for steel C45 (Fig. 11), the duration of the brittle fracture zone is approximately 0,15 ms.

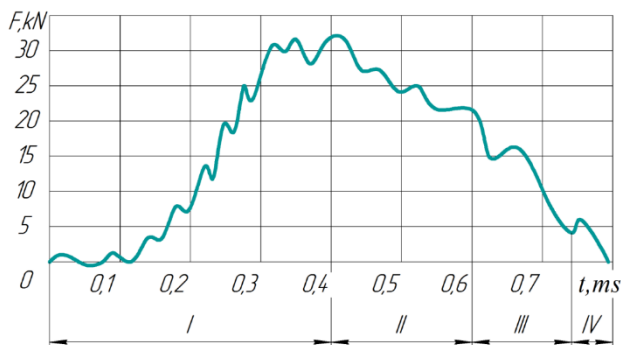


**Fig. 11. Zones of crack propagation under dynamic loading of specimens from steel C45 according to the three-point bending scheme ( $F_4 = f(t)$ )**

This allows to estimate with sufficient accuracy the average velocity of a brittle crack propagation (the crack penetration trajectory was determined from the fracture of the fractured specimen (see Fig. 7)), which was approximately 80 m/s.

The duration of the brittle crack breakthrough for other steel grades was determined in a similar way, which is  $t \cong 0,1 \dots 0,8 \text{ ms}$ . Including average rates of brittle cracks propagation: 60Si7 – 120 m/s; 37Cr4 – 70 m/s; C20 – 50 m/s.

Analysis of the brittle cracks breakthrough rates values shows that they are practically the same under dynamic and static-dynamic loading and do not reach critical values, and therefore the quality of the separated workpieces is quite high.

## CONCLUSIONS

1. Combined static-dynamic loading during cold breaking by bending allows to reduce high-frequency vibrations of the «tool – specimen – support» system, and also to eliminate the violation of the specimen contact with the supports, to reduce the peak values of the forces from the side of the punch and supports.

2. The presence of a static force at the moment of impact provides a certain initial level of tensile stresses in the zone of the stress concentrator, which increases crack controllability. It is assumed that a fracture crack will always propagate in the area of tensile stresses, which improves the quality of the workpieces being separated. A more noticeable improvement in the quality of the workpieces will manifest itself when separating specimens of large cross-sections.

3. The reactive forces from the side of supports from the static force action coincide with the direction of the inertial forces of the specimen halves and additionally break the specimen. In this case, with an increase in the specimen length, the value of its separation from the supports in the initial phase of loading decreases, which has a positive effect on the quality of the obtained workpieces.

4. The magnitude of the static force required to eliminate the separation of the specimen from the supports depends on the stiffness of the contact between the head and the intermediate punch and increases with the increase in the stiffness of the contact between the head and the intermediate punch. The contact stiffness value between the head and the intermediate punch should be selected as optimal one due to the special design of the punch.

5. The obtained experimental results confirm the adequacy of the specimen separation mathematical model by the breaking method under dynamic and static-dynamic loading. It has been experimentally established that the value of the preliminary static force must be at least 40% of the force at which the specimen is failed.

6. Analysis of the values for the brittle cracks breakthrough rates shows that they are practically the same under dynamic and static-dynamic loading and are, respectively: 60Si7 – 120 m/s; C45 – 80 m/s; 37Cr4 – 70 m/s; C20 – 50 m/s. The crack velocities do not reach critical values, and therefore the quality of the separated workpieces is quite high.

7. The obtained results can be used to improve the technology of the separating rolled stock into dimensional workpieces by the method of cold breaking bending.

## SUMMARY

The aim of the work is to improve the quality of workpieces obtained by breaking rolled stock products by researching the separation process under dynamic and static-dynamic loading on a press-hammer. Combined static-dynamic loading during cold breaking by bending allows to reduce high-frequency vibrations of the “tool – specimen – support” system, to eliminate the violation of the contact of the specimen with the supports, to reduce the peak values of the forces from the side of the hatchet and supports. The static force at the moment of impact provides a certain initial level of tensile stresses in the area of the stress concentrator. This has a positive effect on the quality of the obtained workpieces. The magnitude of the static force required to exclude the separation of the specimen from the supports depends on the stiffness of the contact between the head and the intermediate punch and increases with increasing this stiffness. The obtained experimental results confirm the adequacy of the mathematical model of specimen separation by the breaking method under dynamic and static-dynamic loading. It has been experimentally established that the value of the preliminary static force must be at least 40% of the force at which the specimen is broken down. Analysis of the brittle cracks breakthrough rates values shows that they are practically the same under dynamic and static-dynamic loading and are, respectively: 60Si7 – 120 m/s; C45 – 80 m/s; 37Cr4 – 70 m/s; C20 – 50 m/s. The crack velocities do not reach critical values, and therefore the quality of the workpieces being separated is quite high. The results obtained results can be used to improve the technology of the separating rolled stock into dimensional workpieces by the method of cold breaking by bending.

Key words: breaking, bending, press-hammer, impact, dynamic loading, static-dynamic loading, rate/velocity, crack, energy, quality, rolled stock, workpiece.

## Bibliography

1. Tang B., Liu Y., Mao H. Investigation of a novel modified die design for fine-blanking process to reduce the die-roll size. *Procedia Engineering*. 2017. №207, P. 1546–1551. doi:10.1016/j.proeng.2017.10.1076.
2. Joun M. S., Jeong S. W., Park Y. T., Hong S. M. Experimental and numerical study on shearing of a rod to produce long billets for cold forging. *Journal of Manufacturing Processes*. 2021. №62. P. 797–805. doi: 10.1016/j.jmapro.2020.12.062.
3. Карнаух С. Г. Розробка штампів для точного відрізання зсувом. *Машинознавство*. 1998. № 3. С. 34–36.
4. Lisunets N. L. Usage of physical and mathematical simulation for improvement of the processes of metal shear cutting. *CIS Iron and Steel Review*. 2019. №17. P. 34–38.
5. Lisunets N. L. Improving the efficiency of the processes of billets manufacture from rolled metal via shift cutting based on simulation. *Chernye Metally*. 2018. №6. P. 31–35.

6. Karnaukh S. G., Markov O. E., Aliieva L. I., Kukhar V. V. Designing and researching of the equipment for cutting by breaking of rolled stock. *International Journal of Advanced Manufacturing Technology*. 2020. №109. P. 2457–2464. doi: 10.1007/s00170-020-05824-7.

7. Zheng Q., Zhuang X., Zhao Z. State-of-the-art and future challenge in fine-blanking technology. *Production Engineering*. 2019. №13. P. 61–70.

8. Karnaukh S. G., Karnaukh D. S. Research of the influence of deformation speed on energy and power adjectives of the process of three-point cold bend breaking and on alignment integrity of raw parts. *Metallurgical and Mining Industry*. 2011. №3. P. 107–114.

9. Карнаух С. Г., Бігунов О. О., Мучник О. Є. Дослідження процесу статико-динамічного навантаження зразків за схемою триточкового холодного ламання згином на прес-молотах. *Машинознавство*. 2000. №12. С. 31–36.

10. Karnaukh S. G., Aliiev I. S. Research of process of division of grade rolling on the measured blanks by method of breaking bend at static and shock loading. *Scientific journals of Vinnitsa national agrarian university. Engineering, energy, transport*. 2021. Vol.112, №1. С. 81–87. doi: 10.37128/2520-6168-2021-1-10.

11. Karnaukh S. G., Markov O. E., Kukhar V. V., Shapoval A. V. Research of the rolled stock separating into workpieces using breaking by bending with dynamic and static-dynamic force. *The International Journal of Advanced Manufacturing Technology*. 2022. №120. P. 2763–2776. doi: 10.1007/s00170-022-08902-0.

12. Karnaukh S. G., Markov O. E., Kukhar V. V., Shapoval A. V. Classification of steels according to their sensitivity to fracture using a synergetic model. *The International Journal of Advanced Manufacturing Technology*. 2022. №119. P. 5277–5287. doi: 10.1007/s00170-022-08653-y.

**Information about the authors:**

**Karnaukh Sergii Grygorovych,**

Candidate of Technical Sciences,

Associate Professor at the Department of Basics of Designing a Machine

Donbass State Engineering Academy

72, Akademichna Str., Kramatorsk, Donetsk region, 84313, Ukraine

**Markov Oleg Yevhenovych,**

Doctor of Technical Sciences

Professor at the Department of Manufacturing Processes Automation

Donbass State Engineering Academy

72, Akademichna Str., Kramatorsk, Donetsk region, 84313, Ukraine